Appendix A Literature search and selection

Systematic database searches. We extracted a preliminary pool of 157 studies from PubMed using the search term: "sign language" AND ((mri OR fmri) OR ("magnetic resonance" imaging OR functional magnetic resonance imaging) OR pet OR "positron emission tomography"). To minimize the risk of overlooking studies that fit our criteria, we repeated this search in Thomson Reuters Web of Science which yielded 6 additional results (see the flow diagram in Appendix B for an overview of the systematic search, screening, and assessment). After automatically removing duplicates, the pool of potentially relevant publications consisted of 163 studies from which we removed 15 records that could already be identified as false positives (case reports, review papers, etc.).

Study selection. Within the remaining set of 148 records, we then identified 21 studies of SL comprehension that reported results contrasting SL stimuli of varying linguistic complexity (ranging from viewing single signs to short sentences to complex discourse) in their native SL with either: (i) an appropriate control condition, such as a video of a still model or a similar matched control including controls for task effects; or (ii) a low-level baseline. These criteria make it possible to include studies that used different tasks in the same data set as the observed activation is always primarily related to SL comprehension given that task-effects were either controlled for (i.e. studies with "control" conditions) or not present as task-free studies where subjects passible viewed stimuli. Because our interest here lay on how SL is processed in deaf subjects who are native or native-like signers,[1] we excluded studies of bimodal bilinguals (i.e. hearing signers) and experimental conditions that did not use natural SL stimuli but auxiliary sign systems (e.g., Signed Polish; Jednoróg et al. 2015) or non-linguistic gesture (e.g., pantomime or pantomime-like actions). Reflecting standard practice in cognitive neuroscience of language, we only included studies were participants were reported to have been right-handed by the original authors. Studies where participants produced signs while in the scanner were excluded. In this context, it is important to note that the ALE method seeks convergence across the whole brain so that including studies with restricted search spaces would inflate the chance of obtaining high values in that region, which is why we excluded studies reporting only results from specific regions of interest (ROI) as well as conjunction analyses. A summary of inclusion and exclusion criteria as well as other key parameters of this meta-analysis is provided in Appendix C which contains our responses to the checklist for neuroimaging meta-analysis compiled and recommended by (Müller et al. 2018).

Inclusion of previously unpublished data. We further contacted via e-mail the corresponding authors of studies that did not report relevant contrasts but fulfilled our other inclusion criteria and inquired whether they would be willing and able to provide information about previously unpublished contrasts from the analyses they report in their publications. We approached 14 corresponding authors and received five positive responses so that we ultimately could include 3 heretofore unpublished contrasts from independent groups of subjects in our

[1] In the context of this study we consider participants "native signers" when the authors of the studies included in our dataset have described them as deaf users of a SL with native or at least highly fluent (i.e. with native-like proficiency). This entails that participants had either acquired a SL from birth or learned said language early in their life and were using the language as their primary or preferred means of communication. Crucially, the have been judged to be highly proficient singers either by formal or informal assessment by the respective experimenters.

data set (see Appendix D). In total, about half of the corresponding authors we contacted responded to our requests, but most were unable to provide relevant information because they either were no longer able to access the respective study's data or were not permitted to share this unpublished information due to policies in place at their respective institutions.

Sign language comprehension dataset. The final pool of studies included in our dataset for the ALE analysis of SL comprehension in deaf singers consisted of 21 studies reporting results from 23 experiments with independent groups of subjects with a total number of 391 foci and 316 subjects (see Appendix D for a summary of the studies in the dataset). From a linguistic point of view, it should furthermore be noted that the experiments in our dataset used stimuli of varying complexity (single signs, sentences, and complex discourse) constructed in 8 typologically different sign languages primarily used by deaf communities in Europe, North America, and Asia.

Inclusion of non-linguistic SLA observation. Given that our main interest here was to determine which regions of the brain are involved in processing the linguistic aspect of SL stimuli as opposed to stimulus properties depending on the visuo-spatial modality in which SL is externalized, we created a third independent dataset based on studies of SLA observation. In the studies in this dataset, hearing participants processed video stimuli in which actors performed manual, facial, and bodily actions in a pantomime-like fashion. Actions in the data set are not limited to manual movements or to the use of different fingers and hand shapes, but also include data from studies investigating modulations of facial expressions and pointing, all of which roughly correspond to the usage of the three major articulators (hands, face, and body) in SL (i.e. they may be considered "sign-like"). Therefore, these stimuli can be expected to trigger a similar neural response to the stimuli observed by deaf signers during SL comprehension in brain regions processing non-linguistic yet possibly modality-specific aspects of SL stimuli (i.e. visuo-spatial aspects of the performed actions as well as social information about the actor), given that plastic reorganization due to deafness has only been shown with regard to the externalization system (i.e. auditory regions and speech-related white-matter tracts; Emmorey et al. 2003; Finkl et al. 2019).

Creation of SLA observation data set. The data in this set of studies of SLA observation was obtained from an independent meta-analysis of action domains by (Papitto et al. 2020) and originally contained 98 studies reporting 103 experiments of the observation of any possible action (e.g., including studies that used videos of actors handling objects, climbing a tree, doing gymnastics, etc.) by right-handed hearing non-signers. We then proceeded to remove studies that used stimuli which were not sign-like in the sense that they did not primarily involve the three major articulators (hands, face, and body) as in producing SL. This primarily concerned removing studies showing the handling of actual objects instead of pantomime-like actions as well as studies with stimuli showing complex actions such as climbing a tree. We also excluded two experiments (Corina et al. 2007; Emmorey et al. 2010) that had used SL stimuli and presented them to non-signers, in order to ensure that any observed similarity between our two data sets is driven by the similarity of non-linguistic processes involved in both, SL comprehension and action observation. The final pool of studies included in our dataset for the ALE analysis of action observation in hearing non-signers consisted of 26 experiments with a total number of 549 foci and 431 subjects (see Appendix E for a summary of the studies in the dataset).

Appendix B Flow diagram of literature search

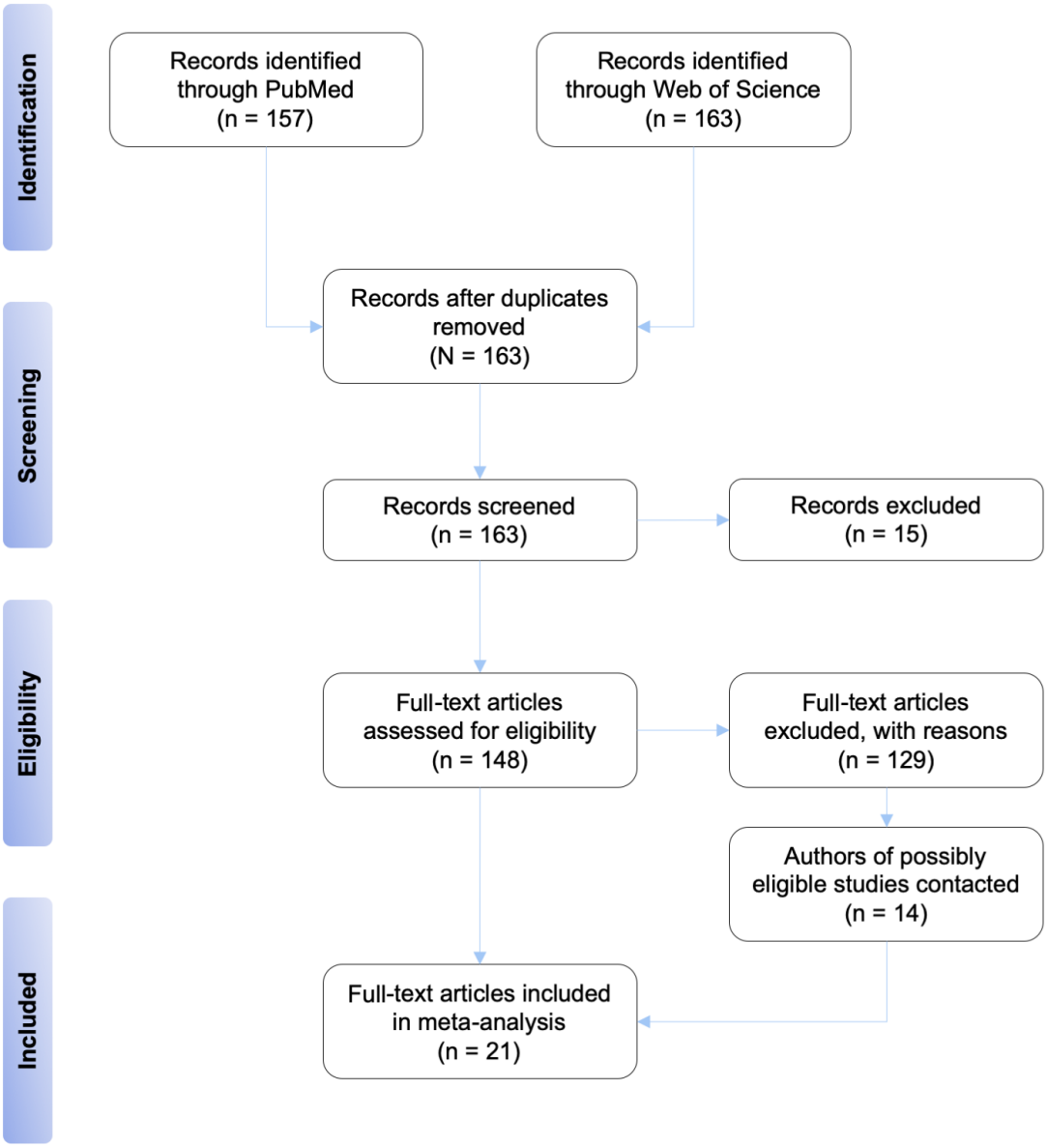

Figure Appendix B. Flow diagram of literature search performed to identify published studies potentially legible for inclusion in our datasets of sign language processing and production. The diagram is modeled on the Preferred Report Items for Systematic Reviews and Meta-Analysis (PRISMA) guidelines (Moher et al. 2009)

Appendix C Checklist for neuroimaging meta-analysis

Checklist for neuroimaging meta-analysis as recommended for inclusion with publications in the guidelines by Müller et al. (2018). The responses for this study have been added in italics to the given statements in the right column.

The research question is specifically defined	YES, and it includes the following contrasts: • *Sign language processing > baseline/control* • *Action observation > baseline/control*
The literature search was systematic	YES, it included the following keyword in the following databases: *"Sign language comprehension" dataset* *We searched PubMed using the term* "sign language" AND ((mri OR fmri) OR ("magnetic resonance" imaging OR functional magnetic resonance imaging) OR pet OR "positron emission tomography"). *To ensure that we did not miss potentially eligible studies we performed a second search using the same term in Web of Science. Duplicates were removed automatically and the remaining results were added to the set of potentially eligible studies. See Appendix A for a flow diagram detailing the literature search.* *"Sign-like action observation" dataset:* *Data were obtained by applying the inclusion and exclusion criteria described below to a pre-existing dataset compiled for a different study (Papitto et al. 2020).*
Detailed inclusion and exclusion criteria are included	*YES, and reasons of non-standard criterion were:* *"Sign language comprehension" dataset* *Inclusion:* • *Deaf signers as subjects, considered as "native signers" by the authors of a study.* • *Subjects were right-handed, according to the authors of a study.* • *Reports a relevant contrast, as defined above.* • *Reports data from whole-brain analysis.* • *Study used stimulus material in a natural sign language, not an auxiliary sign system or non-linguistic gesture.* • *Signers were either performing a task or viewing the stimulus material passively.* *Exclusion:* • *Subjects are hearing signers or non-signers.* • *Subjects were not right-handed.* • *Study does not report a relevant contrast.* • *Search space was limited (i.e. ROI analysis).* • *Study was not conducted using natural sign language stimuli.*

	• *Signers produced signs while in the scanner.* *<u>"Sign-like action observation" dataset:</u>* *Inclusion:* • *Videos of manual, facial, and/or bodily actions were viewed either while performing a task or passively.* • *Subjects were healthy and hearing (if not explicitly reported by the authors of a study, this was assumed to be the default).* • *Subjects were right-handed.* *Exclusion:* • *Subjects were not right-handed.* • *Stimuli showed signs of a natural sign language.* • *Stimuli videos showed handling of actual objects.*
Sample overlap was taken into account	YES, using the following method: *1) Foci data was organized according to sample (subject group) and not experimental contrast.* 2) *Publications were checked for references to previously publications with the same sample.*
All experiments use the same search coverage (state how brain coverage is assessed and how small volume corrections and conjunctions are taken into account)	YES, the search coverage is the following: *We only included contrasts of whole-brain analyses. ROI analyses and conjunction analyses were disregarded.*
Studies are converted to a common reference space	YES, using the following conversion(s): *Talairach space was transformed to MNI space using Lancaster transform as implemented in the GingerALE toolbox (version 2.3.6).*
Data extraction have been conducted by two investigators (ideal case) or double checked by the same investigator (state how double-checking was performed)	YES, the following authors: • *PCT checked inclusion criteria.* • *PCT and GP extracted coordinates.* • *PCT and GP extracted other info: study metadata (e.g, number of subjects, information about paradigms, etc.).* • *PCT, GP and two student assistants double-checked the following data: foci data and study metadata.*
The paper includes a table with at least the references, basic study description (e.g., for fMRI task: stimuli), contrasts and basic sample descriptions (e.g., size, mean age and gender distribution, specific characteristics) of the included studies, source of information (e.g. contact with authors), reference space	YES, and also the following data: *See Appendix S and Appendix T for tables summarizing the relevant information for all datasets. Studies have been organized according to method used (fMRI or PET), sample size (number of subjects), task, contrast(s) included in the analysis, coordinate space used in the original paper for reporting results (Talairach or MNI), and number of peaks. For the sign language comprhension dataset, we also report the language used as stimulus material.*
The study protocol was previously registered and all analyses planned beforehand, including the methods and	*IN PART*:

parameters used for inference, correction for multiple testing, etc.	*1) This study was not registered before starting the search, yet inclusion and exclusion criteria listed above were defined beforehand against the background of explicit linguistic considerations.* *2) Any non-planned analyses are clearly stated as post-hoc or non-prespecified in the paper.* 3) *The meta-analysis used the default methods and parameters of the software, with the following exceptions: No known exceptions, details listed in methods section.*
The meta-analysis includes diagnostics	YES, the following: *Mass-overlap analyses, lateralization analyses, and meta-analytic connectivity modeling.*

Appendix D Summary of sign language (SL) comprehension studies

Study	Method	Subjects (N)	Task	Contrast	Language	Coordinate space	Peaks (N)
(Capek et al. 2008)	fMRI	13	Target-detection	Manual-only signs > control	British Sign Language	Talairach	4
				Signs > control			3
				Signs with echo phonology > control			5
(Cardin et al. 2013) *	fMRI	15	Target-detection	Sign language > baseline	British Sign Language	MNI	10
		16		Sign language > baseline	Svenskt teckenspråk (Swedish Sign Language)	MNI	11
(Corina et al. 2007)	PET	10	Recognition task (similar to Sternberg)	Sign language > control	American Sign Language	MNI	20
(Emmorey et al. 2010)	fMRI	14	Passive viewing	Signs > baseline	American Sign Language	MNI	6
(Gizewski et al. 2005)	fMRI	12	Passive viewing	Sing language discourse > baseline	Deutsche Gebärdensprache (German Sign Language)	MNI	4
(Inubushi and Sakai 2013)	fMRI	28	Lexical decision	Sign > control	Nihon Shuwa (Japanese Sign Language)	MNI	3
			Grammaticality judgement	Sentence > control			12
			Discourse coherence judgement	Discourse > control			14
(Jednoróg et al. 2015)	fMRI	15	Passive viewing	Sign language > baseline	Polski Język Migowy (Polish Sign Language)	Talairach	16
				Classifier constructions > baseline			15
(Malaia et al. 2012)	fMRI	14	Passive viewing	Sign language > baseline	American Sign Language	MNI	5
(Mayberry et al. 2011)	2011	22	Grammaticality judgement	Sentence > baseline	American Sign Language	MNI	8
			Phoneme judgement	Sentence > baseline			13
(McCullough et al. 2012) *	fMRI	12	Target-detection	Motion sentences > control	American Sign Language	Talairach	5
				Static sentences > control			7
(McGuire et al. 1997)	PET	5	Covert sentence completion	Covert sign > control	British Sign Language	Talairach	4
(MacSweeney et al. 2002)	fMRI	9	Target detection	Sign language > control	British Sign Language	Talairach	11

(MacSweeney et al. 2004)	fMRI	9	Target-detection	Sign language > control	British Sign Language	Talairach	8
(MacSweeney et al. 2006)	fMRI	9	Target-detection	Sentence > control	British Sign Language	Talairach	7
				List > control			11
(MacSweeney et al. 2008)	fMRI	20	Rhyming task	Location > control	British Sign Language	Talairach	3
(Moreno et al. 2018)	fMRI	20	Passive viewing	Sentence > list	Langue des Signes Française (French Sign Language)	MNI	10
(Newman et al. 2015)	fMRI	19	Picture-video matching (similar to Sternberg)	Motion classifier construction > baseline	American Sign Language	MNI	35
				Motion classifier construction > control			15
(Newman et al. 2010)	fMRI	14	Semantic recognition	Sentence (without inflectional morphology) > control	American Sign Language	MNI	12
				Sentence (with inflectional morphology) > control			19
(Petitto et al. 2000)	PET	5	Passive viewing	Lexical signs > baseline	American Sign Language	Talairach	18
		6		Lexical signs > baseline	Langue des Signes Québécoise (Quebec Sign Language)		30
(Trumpp and Kiefer 2018)	fMRI	16	Passive viewing	Sign language > baseline	Deutsche Gebärdensprache (German Sign Language)	MNI	43
(Waters et al. 2007)	fMRI	13	Target-detection	Sign language > control	British Sign Language	Talairach	4
Total		**316**					**391**

Table Appendix D. Summary of studies of SL. Studies have been organized according to method used (fMRI or PET), sample size (number of subjects), task, contrast(s) included in the analysis ("control" indicating that the study was controlled for stimulus and task effects; "baseline" indicating that the study used a [low-level] baseline such as a still model or a fixation cross), language used as stimuli, coordinate space used in the original paper for reporting results (Talairach or MNI), and number of peaks. An asterisk (*) next to the author names indicates studies where relevant contrast information is not part of the published paper but was provided by the respective study's corresponding author upon request via e-mail. See the online materials for a list of peak locations as reported by the authors of the respective study (filename: "sign_language_processing.txt"). Petitto et al. (2000) and Cardin et al. (2013) present two studies of different sign languages with independent groups in a single paper, consequently the table lists 21 papers, but 23 experiments actually entered into this ALE analysis.

Appendix E Summary of sign-like action (SLA) observation studies

Study	Method	Subjects (N)	Task	Contrast	Coordinate space	Peaks (N)
(Adamovich et al. 2009)	fMRI	13	Observe action to imitate later	Observe > baseline	MNI	24
(Buccino et al. 2001)	fMRI	12	Passive observation	Action observation > control	Talairach	2
(Carr et al. 2003)	fMRI	11	Passive observation	Action observation > baseline	Talairach	22
(Corina et al. 2007)	PET	10	Passive observation	Self-oriented action > baseline	MNI	23
				Object-oriented action > baseline		19
(Emmorey et al. 2010)	fMRI	14	Passive observation	Pantomimes > baseline	MNI	22
(Engel et al. 2008)	fMRI	18	Passive observation	Moving hand > control	MNI	20
(Georgescu et al. 2014)	fMRI	21	Passive observation	Action observation > control	MNI	20
(Grosbras and Paus 2006)	fMRI	20	Passive observation	Hand > control	MNI	25
				Angry hand > control		32
				Neutral face > control		28
				Angry face > control		27
(Handjaras et al. 2015)	fMRI	14	Passive observation	Intransitive action observation > baseline	Talairach	12
				Transitive action observation > baseline		10
(Horan et al. 2014)	fMRI	23	Passive observation	Observe fingers > baseline	MNI	14
(Kilintari et al. 2016)	fMRI	14	Observe action to imitate later	Action observation > baseline	MNI	40
(Li et al. 2015)	fMRI	30	Passive observation	Action observation > control	MNI	2
(Lorey et al. 2013)	fMRI	15	Passive observation	Action observation > baseline	MNI	9
(Martineau et al. 2010)	fMRI	8	Passive observation	Action observation > baseline	MNI	3
(Montgomery et al. 2007)	fMRI	14	Observe action to imitate later	Hand pantomime > baseline	Talairach	16
				Hand pantomime > baseline		16
(Montgomery and Haxby 2008)	fMRI	12	Observe action to imitate later	Observe facial expressions > baseline	Talairach	16
				Observe hand gestures > baseline		11
(Pierno et al. 2009)	fMRI	15	Passive observation	Pointing > control	MNI	4
(Plata Bello et al. 2013)	fMRI	19	Passive observation	Index-thumb > control	MNI	21
				Middle-thumb > control		6
				Ring-thumb > control		3
				Little-thumb > control		5
(Plata Bello et al. 2014)	fMRI	31	Passive observation	Action observation > control	MNI	14
(Plata-Bello et al. 2017)	fMRI	15	Passive observation	Action observation > control	MNI	3
(Sperduti et al. 2014)	fMRI	23	Passive observation	Hand action observation > baseline	MNI	13

(Szameitat et al. 2012)	fMRI	21	Passive observation	Hand action observation > baseline	MNI	4
(Villarreal et al. 2008)	fMRI	17	Gesture category recognition task	Gestures > baseline	Talairach	24
				Meaningless gesture > baseline		29
(Wheaton et al. 2004)	fMRI	12	Passive observation	Face moving > baseline	Talairach	5
				Hand moving > baseline		5
Total		**431**				**549**

Table Appendix E. Summary of studies of SLA observation. Studies have been organized according to method used (fMRI or PET), sample size (number of subjects), task, contrast(s) included in the analysis, coordinate space used in the original paper for reporting results (Talairach or MNI), and number of peaks. See the online materials for a list of peak locations as reported by the authors of the respective study (filename: "action_observation.txt").

Appendix F Anatomical Volumes of Interest in bilateral IFG

Anatomical VOI were created using the maximum probability maps for bilateral area 44 and 45 (Amunts et al. 1999) available as part of the SPM Anatomy Toolbox (Eickhoff et al. 2005, 2007). These maps are derived from mappings of 10 postmortem brains and probabilistic in nature due to considerable between-subject variability in cytoarchitecture. The default maps which can be exported from the Anatomy Toolbox using the GUI are thresholded in a way that avoids any overlap between area 44 and 45. Because our analysis was based on data analyzed using different software packages and reported in different coordinate spaces that were transformed into MNI space with a resolution of 2x2x2 mm, we sought to account for the inevitable reduction in spatial precision by using the cytoarchitectonic maximum probability maps without avoiding overlap between area 44 and 45. While this results in rather liberal definitions of area 44 and 45 in direct comparison to stereological volume measured in postmortem data at micrometer histological resolution, a similar strategy has been employed in a number of meta-analytic structure-to-function mappings (e.g., Clos, Amunts, Laird, Fox, & Eickhoff, 2013). Our VOIs thus include only those voxels which are likely to represent either cytoarchitectonic area 44, area 45 or a composite of the two. They were created by extracting the raw probability maps shipped with the Anatomy Toolbox, normalizing them to match the standard space of our template brain (Colin27_T1_seg_MNI_2x2x2.nii), and binarizing these maps. This yielded two separate anatomical masks for area 44 and 45 based on cytoarchitectonic mappings with an overlap of voxels between masks of 22.13 % in the left and 25.86 % in the right hemisphere (see Figure below). In addition, we created a composite mask for Broca's region and its right-hemispheric homologue containing all voxels in the brain that were cytoarchitectonically likely to represent area 44 and/or area 45.

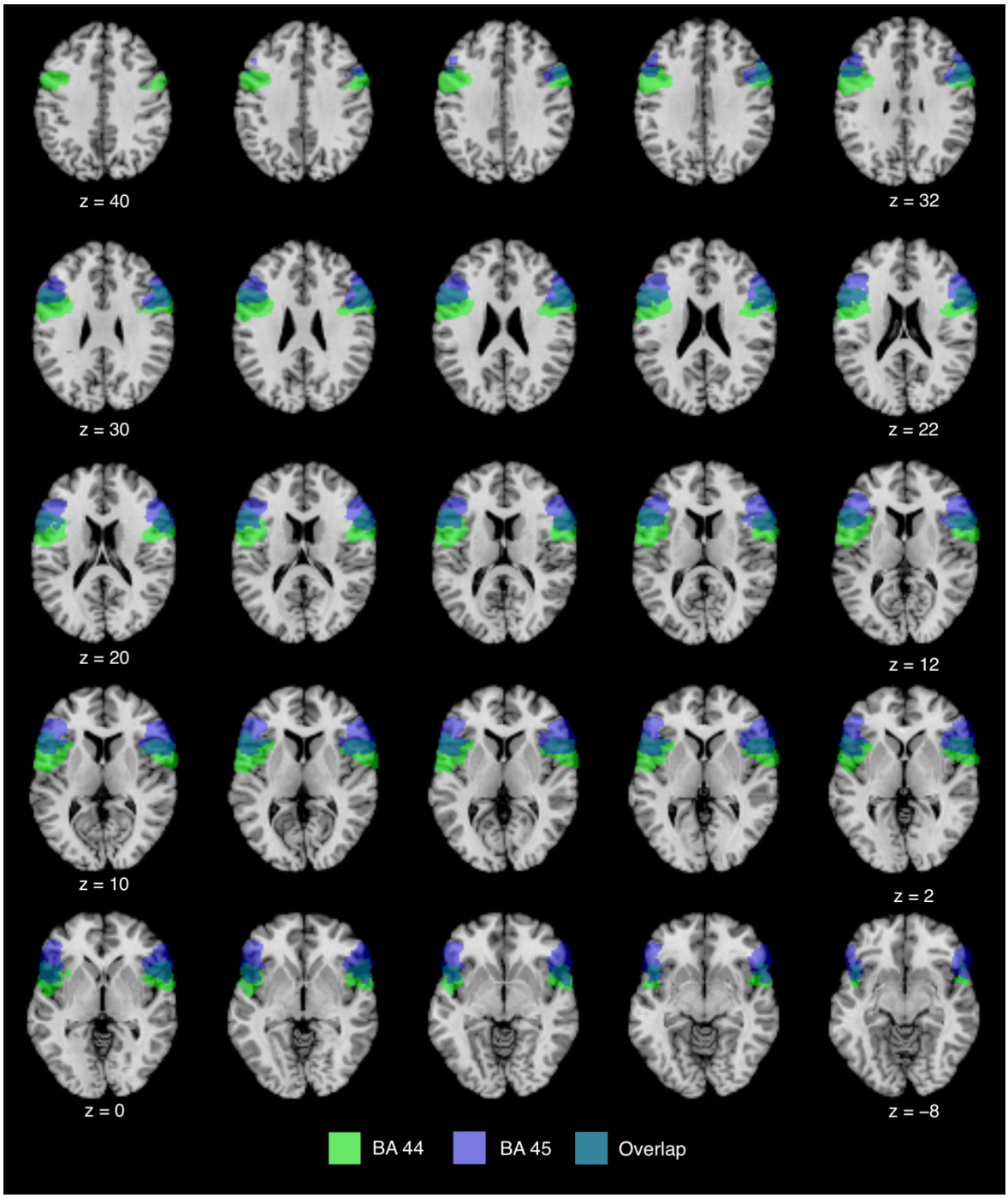

Figure Appendix F. Anatomical VOI based on cytoarchitectonic mappings of IFG. Range of axial slices from z = 40 to x = -8 with overlays of maximum probability maps for area 44 (green) and area 45 (blue) in both hemispheres from the SPM Anatomy Toolbox. Overlap between maps in the anterior part of area 44 and the posterior part of area 45 indicated in cyan. Slices taken from a template brain (Colin27_T1_seg_MNI_2x2x2.nii).

Appendix G ALE results for SL comprehension dataset

Cluster	Hemisphere	Brain region	BA	MNI Coordinates (mm)			ALE Score (× 10^{-2})	Cluster Size (mm^3)
				x	y	z		
1	Left	Inferior frontal gyrus	44	-48	12	28	3.30	5,240
	Left	Inferior frontal gyrus	45	-50	20	14	2.53	
2	Right	Middle temporal gyrus	37	50	-66	2	3.27	2,392
	Right	Inferior temporal gyrus	37	48	-60	-10	1.91	
3	Right	Inferior frontal gyrus	45	56	18	22	2.58	2,296
	Right	Inferior frontal gyrus	45	52	22	16	1.94	
	Right	Inferior frontal gyrus	45	48	26	2	1.66	
4	Left	Middle occipital gyrus	19	-50	-74	4	2.37	2,072
5	Right	Superior temporal gyrus	22	48	-36	6	2.55	1,776
6	Left	Precentral gyrus	6	-42	2	58	2.30	1,216
	Left	Middle frontal gyrus	8	-40	12	46	1.57	
7	Left	Insula lobe	13	-32	20	4	1.84	1,040
	Left	Insula lobe	13	-36	20	2	1.76	

Table Appendix G. Spatial convergence for "SL comprehension > control/baseline" contrasts. Functional clusters obtained from ALE analysis, identifying regions with functional convergence for SL comprehension. The GingerALE output for this analysis is available as part of the online materials. Mask dimensions = 77 x 96 x 79; number of within-brain voxels = 229,781; number of foci = 391; number of experiments = 23; total number of subjects = 316; maximum ALE score (× 10-2) = 3.30; thresholding method = cluster-level inference; thresholding value = .05; number of thresholding permutations = 10,000; cluster-forming value = .001.

Appendix H Results of mass overlap analysis in IFG

	Number of voxels from left IFG cluster	Number of voxels from right IFG cluster
Area 44	515	131
Area 45	385	282
Intersection	291	131
Broca's area / Area 44 and 45	609	282

Table Appendix H. Results of mass overlap analysis in IFG. Total number of voxels for the clusters in left and right IFG from the convergence map for SL comprehension that fall into cytoarchitectonically defined area 44, area 45, and a composite mask of both defining Broca's area.

Appendix I Replication of mass overlap analysis in IFG with non-intersecting VOI

Because the cytoarchitectonic masks used in the mass overlap analysis reported in the main text use rather liberal thresholds, we provide this replication of our analysis using conservatively thresholded anatomical VOI.

The functional convergence map obtained from the ALE analysis of the SL comprehension dataset was used to perform a mass overlap analysis in bilateral IFG to explore the sub-regional spatial distribution for significant clusters. We used cytoarchitectonically defined VOIs covering area 44 and area 45 bilaterally (Amunts et al. 1999) extracted from the SPM Anatomy Toolbox (Eickhoff et al. 2005, 2007), as well as a composite mask of Broca's area (area 44 and 45). These default maps were exported from the Anatomy Toolbox using the GUI and are thresholded in way that avoids any overlap between both area 44 and area 45. Because the output of GingerALE uses 2x2x2 mm as default voxel size, the masks were binarized and resliced to fit the dimensions of the ALE convergence map. To determine the mass overlap between significant clusters for SL comprehension and area 44 and area 45, the respective VOIs were then multiplied with the left or right IFG clusters extracted from the convergence map from the ALE analysis of the SL comprehension dataset.

Of the whole activation mass found in left inferior frontal cortex in the convergence map for SL comprehension, a proportion of 31.60 % fell into the anatomical mask for Broca's area. In right IFG, 53.66 % of total activation mass in IFG fell into the combined map of area 44 and area 45. For the activation mass within Broca's area 56.52 % could be assigned to cytoarchitectonic area 44 and 43.48 % to cytoarchitectonic area 45 (see Table below). In the homologous right-hemispheric regions, 92.86 % could be assigned to area 45 and 7.14 % to area 44. In sum, these results replicate the observation from our original analyses, as the observed spatial convergence across studies in bilateral IFG in the ALE analysis can only be attributed to cytoarchitectonically defined area 44 in the left but not the right hemisphere.

	Number of voxels from left IFG cluster	Number of voxels from right IFG cluster
Area 44	117	11
Area 45	90	143
Broca's area / Area 44 and 45	207	154

Table Appendix I. Results of the replication of mass overlap analysis in IFG using the non-intersecting more conservatively thresholded VOI that can be extracted by default from the SPM Anatomy Toolbox. Total number of voxels for the cluster in left and right IFG from the convergence map for SL comprehension that fall into cytoarchitectonically defined area 44, area 45, and a composite mask of both defining Broca's area.

Appendix J ALE results for SLA observation dataset

Cluster	Hemisphere	Brain region	BA	MNI Coordinates (mm)			ALE Score ($\times 10^{-2}$)	Cluster Size (mm^3)
				x	y	z		
1	Right	Middle temporal gyrus	37	48	-70	4	4.31	9,664
	Right	Middle temporal gyrus	21	56	-42	4	3.67	
	Right	Superior temporal gyrus	40	58	-34	22	2.45	
2	Left	Inferior occipital gyrus	19	-44	-70	-8	3.47	7,128
	Left	Middle temporal gyrus	19	-52	-68	8	3.13	
	Left	Middle temporal gyrus	21	-56	-50	6	3.09	
	Left	Middle occipital gyrus	19	-42	-80	-2	1.96	
3	Right	Precentral gyrus	6	56	4	42	3.39	6,208
	Right	Inferior frontal gyrus	44	56	16	10	2.69	
	Right	Inferior frontal gyrus	44	52	12	26	2.64	
	Right	Inferior frontal gyrus	45	52	18	24	2.32	
4	Left	Inferior parietal lobule	7	-36	-48	52	3.72	5,656
	Left	Postcentral gyrus	40	-38	-36	50	3.48	
	Left	Superior parietal lobule	7	-26	-60	52	1.62	
5	Left	Precentral gyrus	6	-52	8	40	4.01	3,112
	Left	Inferior frontal gyrus	44	-54	8	24	1.71	
6	Right	Inferior parietal lobule	7	40	-50	52	2.27	1,992
	Right	Superior parietal lobule	7	34	-52	62	1.84	
	Right	Inferior parietal lobule	7	30	-52	54	1.74	
	Right	Superior parietal lobule	7	32	-64	50	1.63	
	Right	Inferior parietal lobule	2	34	-38	50	1.50	

Table Appendix J. Spatial convergence for "SLA observation > control/baseline" contrasts. Functional clusters obtained from ALE analysis identifying regions with functional convergence for non-linguistic SLA observation by hearing non-signers. The GingerALE output for this analysis is available as part of the online materials. Mask dimensions = 77 x 96 x 79; number of within-brain voxels = 229,781; number of foci = 549; number of experiments = 26; total number of subjects = 431; maximum ALE score (× 10-2) = 4.31; thresholding method = cluster-level inference; thresholding value = .05; number of thresholding permutations = 10,000; cluster-forming value = .001.

Appendix K Contrast analysis: SLA observation > SL comprehension

Cluster	Hemisphere	Brain region	BA	MNI Coordinates (mm)			Z Score	Cluster Size (mm^3)
				x	y	z		
1	Left	Superior parietal lobule	7	-33.2	-55.2	60	3.72	4,032
	Left	Inferior parietal lobule	7	-30	-46	54	3.54	
	Left	Superior parietal lobule	7	-30	-50	56	3.35	
	Left	Inferior parietal lobule	40	-38	-52	50	2.99	
	Left	Inferior parietal lobule	40	-40	-40	50	2.83	
	Left	Postcentral gyrus	1	-40	-32	52	2.74	
	Left	Inferior parietal lobule	40	-40	-46	46	2.65	
	Left	Inferior parietal lobule	40	-46	-40	48	2.60	
2	Left	Precentral gyrus	44/6	-57.9	4.6	40.2	3.72	1,912
3	Right	Middle temporal gyrus	37	54	-48	6	2.99	1,824
4	Right	Inferior temporal gyrus	19	40	-66	-6	2.56	1,368
	Right	Middle occipital gyrus	19	42	-72	6	2.49	
5	Left	Middle temporal gyrus	21	-60	-50	8	2.60	896
	Left	Middle temporal gyrus	39	-58	-56	8	2.39	
6	Right	Inferior frontal gyrus	44	56	16	6	2.65	784
7	Left	Inferior occipital gyrus	19	-38	-68	-4	2.64	768
8	Right	Superior parietal lobule	7	32	-50	58	2.88	680
	Right	Superior parietal lobule	7	38	-48	60	2.69	
9	Right	Inferior frontal gyrus	44	50	6	26	2.56	592
10	Right	Superior temporal gyrus	40	58	-38	22	2.16	496
11	Right	Precentral gyrus	6	56	0	46	2.79	384

Table Appendix K. SLA observation > SL comprehension. Significant clusters for SLA observation after subtracting SL comprehension. The GingerALE output for this analysis is available as part of the online materials. Mask dimensions = 77 x 96 x 79; number of within-brain voxels = 229,781; thresholding method = uncorrected p-value; thresholding value = .05; volume > threshold = 3,872 mm3; minimum cluster size = 100 mm3.

Appendix L Conjunction: SL comprehension ∧ SLA observation

Cluster	Hemisphere	Brain region	BA	MNI Coordinates (mm)			ALE Score ($\times 10^{-2}$)	Cluster Size (mm^3)
				x	y	z		
1	Right	Middle temporal gyrus	19	50	-66	2	3.27	1,896
	Right	Inferior temporal gyrus	37	48	-62	-8	1.81	
2	Left	Middle temporal gyrus	19	-50	-72	6	2.25	1,400
	Left	Inferior Occipital gyrus	19	-50	-70	-2	1.83	
3	Right	Inferior frontal gyrus	45	54	20	22	2.17	1,096
4	Right	Middle temporal gyrus	21	50	-40	4	1.87	456
5	Left	Precentral gyrus	44/6	-50	10	34	2.07	352

Table Appendix L. Conjunction of SL comprehension and SLA observation convergence maps. Overlap of voxels in significant clusters observed for SL comprehension with those observed for SLA observation. The GingerALE output for this analysis is available as part of the online materials. Mask dimensions = 77 x 96 x 79; number of within-brain voxels = 229,781.

Appendix M Functional domains in BrainMap for SL-specific left IFG cluster

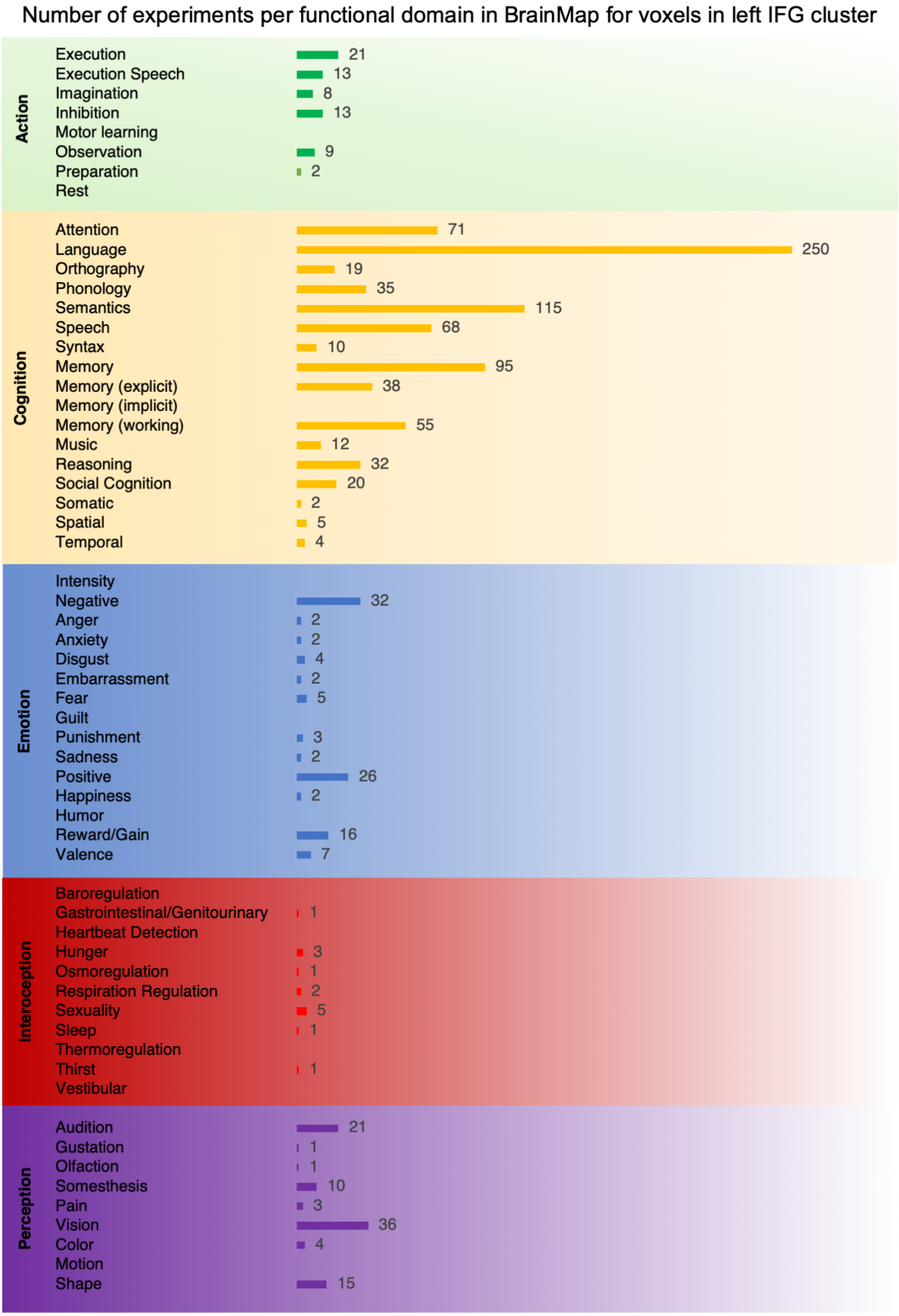

Figure Appendix M. Functional domains in the BrainMap database (containing the results of 3,406 papers describing 16,901 experiments at the time of search) associated with voxels in the SL-specific left IFG cluster from the SL comprehension vs. SLA observation contrast analysis. Voxels that are part of this cluster that were specifically observed during SL comprehension across studies were also activated in experiments attributed to the five given major domains and sub-domains. The graph indicates the total number of experiments that have been associated with a domain. The Sleuth output for this analysis is available as part of the online materials.

Appendix N Meta-analytic connectivity of SL-specific left IFG cluster

Cluster	Hemi-sphere	Brain region	BA	MNI Coordinates (mm)			ALE Score ($\times 10^{-2}$)	Cluster Size (mm^3)
				x	y	z		
1	Left	Inferior frontal gyrus	44	-46	14	24	55.36	56,512
	Left	Insula lobe	13	-34	24	-2	20.66	
	Left	Precentral gyrus	6	-44	4	46	15.38	
	Left	Middle frontal gyrus	10	-36	50	12	10.17	
2	Right	Insula lobe	13	36	22	-4	16.44	29,912
	Right	Inferior frontal gyrus	45	48	14	26	15.25	
	Right	Inferior frontal gyrus	45	48	28	20	12.43	
	Right	Middle frontal gyrus	6	42	2	54	6.89	
	Right	Middle frontal gyrus	6	32	6	54	6.74	
3	Left	Fusiform gyrus	37	-40	-60	-14	11.94	22,072
	Left	Middle temporal gyrus	21	-56	-44	2	11.27	
	Left	Middle temporal gyrus	22	-58	-14	-2	7.05	
	Left	Cerebellum		-42	-56	-30	6.23	
	Left	Middle occipital gyrus	18	-32	-86	6	5.28	
4	Left	Posterior-medial frontal	8	-2	20	46	25.91	21,656
5	Left	Superior parietal lob-ule	7	-28	-62	48	17.88	17,712
	Left	Inferior parietal lobule	39	-32	-54	48	16.92	
6	Left	Sublobar (unassigned)		-14	4	8	10.58	7,232
	Left	Thalamus	50	-8	-14	6	9.03	
7	Right	Inferior parietal lobule	39	38	-52	48	12.09	7,072
8	Right	Cerebellum		36	-66	-24	9.54	4,072
	Right	Inferior temporal gyrus	37	50	-64	-8	7.35	
	Right	Fusiform gyrus	37	38	-52	-20	7.28	
9	Right	Thalamus	50	10	-12	2	8.22	3,256
	Right	Caudate nucleus	48	12	10	8	7.06	
	Right	Sublobar (unassigned)		16	2	12	5.69	
	Right	Putamen	49	22	6	4	5.46	
10	Right	Middle temporal gyrus	21	54	-34	2	10.00	2,048
11	Right	Inferior occipital gyrus	18	28	-90	-6	7.26	1,784

Table Appendix N. Meta-analytic functional connectivity of SL-specific left IFG cluster. Functional clusters obtained by MACM for left IFG cluster from the SL comprehension vs. SLA observation contrast, identifying regions that are co-activated with voxels in this SL-specific cluster in all functional studies in the BrainMap database (containing the results of 3,406 papers describing 16,901 experiments at the time of search). The GingerALE output for this analysis is available as part of the online materials. Mask dimensions = 77 x 96 x 79; number of within-brain voxels = 229,781; number of foci = 6,392; number of experiments = 363; total number of subjects = 5,448; maximum ALE score (× 10-2) = 55.36; thresholding method = cluster-level inference; thresholding value = .05; number of thresholding permutations = 10,000; cluster-forming value = .001.

Appendix O Functional domains in BrainMap for SL-specific right STG cluster

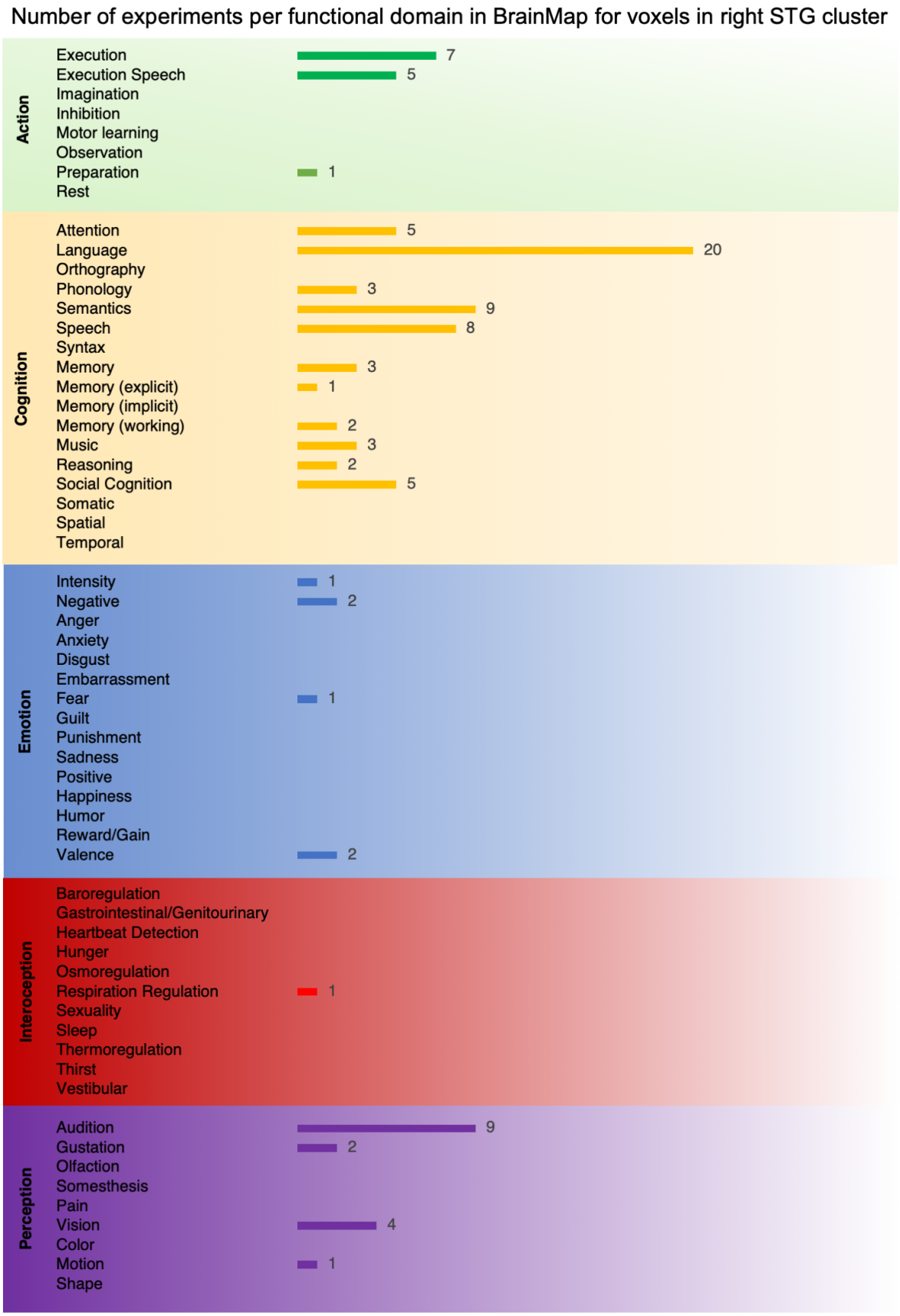

Figure Appendix O. Functional domains in the BrainMap database (containing the results of 3,406 papers describing 16,901 experiments at the time of search) associated with voxels in the SL-specific right STG cluster from the SL comprehension vs. SLA observation contrast analysis. Voxels that are part of this cluster observed during SL comprehension were also activated in experiments attributed to the five given major domains and sub-domains. The graph indicates the total number of experiments that have been associated with a domain. The Sleuth output for this analysis is available as part of the online materials.

Appendix P Meta-analytic connectivity of SL-specific right STG cluster

Cluster	Hemi-sphere	Brain region	BA	MNI Coordinates (mm)			ALE Score ($\times 10^{-2}$)	Cluster Size (mm^3)
				x	y	z		
1	Right	Superior temporal gyrus	22	48	-32	4	12.42	7,728
2	Left	Middle temporal gyrus	21	-60	-32	4	2.71	4,360
	Left	Superior temporal gyrus	22	-60	-22	2	2.36	
	Left	Middle temporal gyrus	22	-60	-14	-2	2.35	
	Left	Superior temporal gyrus	22	-48	-34	8	2.19	
	Left	Superior temporal gyrus	22	-56	-8	-2	2.08	
3	Left	Fusiform gyrus	37	-42	-60	-18	3.18	1,512
4	Left	Postcentral gyrus	4	-48	-6	40	2.64	1,504
5	Left	Inferior frontal gyrus	45	-58	18	18	2.40	1,472
	Left	Inferior frontal gyrus	45	-50	26	14	2.35	
6	Left	Inferior occipital gyrus	19	-40	-70	-8	2.50	1,456
	Left	Inferior occipital gyrus	18	-36	-84	-6	2.37	
7	Right	Posterior-medial frontal	6	6	4	62	2.34	1,096
	Left	Posterior-medial frontal	6	-2	4	60	2.22	
8	Right	Inferior frontal gyrus	44	46	8	24	2.31	880
	Right	Inferior frontal gyrus	45	42	10	30	2.25	

Table Appendix P. Meta-analytic functional connectivity of SL-specific right STG cluster. Functional clusters obtained by MACM for SL-specific right STG cluster from the SL comprehension vs. SLA observation contrast, identifying regions that are co-activated with voxels in this cluster in all functional studies in the BrainMap database (containing the results of 3,406 papers describing 16,901 experiments at the time of search). The GingerALE output for this analysis is available as part of the online materials. Mask dimensions = 77 x 96 x 79; number of within-brain voxels = 229,781; number of foci = 754; number of experiments = 35; total number of subjects = 499; maximum ALE score (× 10-2) = 12.42; thresholding method = cluster-level inference; thresholding value = .05; number of thresholding permutations = 10,000; cluster-forming value = .001.

Appendix Q Functional domains in BrainMap for SL-specific left MFG/PCG cluster

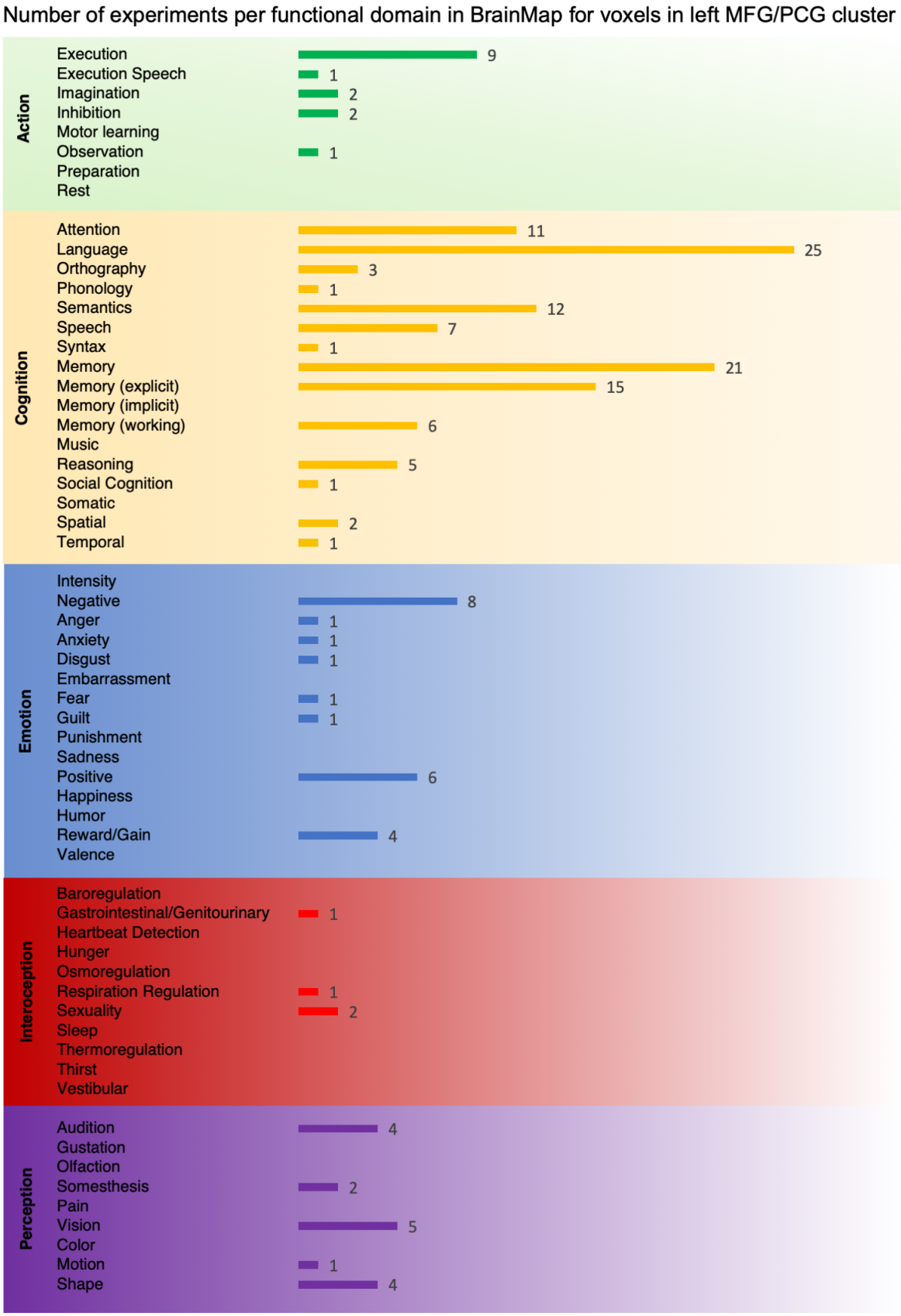

Figure Appendix Q. Functional domains in the BrainMap database (containing the results of 3,406 papers describing 16,901 experiments at the time of search) associated with SL-specific voxels in the SL-specific left MFG/PCG cluster from the SL comprehension vs. SLA observation contrast analysis. Voxels that are part of this cluster observed during SL comprehension were also activated in experiments attributed to the five given major domains and sub-domains. The graph indicates the total number of experiments that have been associated with a domain. The Sleuth output for this analysis is available as part of the online materials.

Appendix R Meta-analytic connectivity of SL-specific left MFG/PCG cluster

Cluster	Hemi-sphere	Brain region	BA	MNI Coordinates (mm)			ALE Score ($\times 10^{-2}$)	Cluster Size (mm^3)
				x	y	z		
1	Left	Precentral gyrus	6	-42	6	50	19.45	14,856
	Left	Precentral gyrus	44	-50	12	30	4.53	
	Left	Middle frontal gyrus	9	-44	30	32	2.14	
2	Left	Posterior-medial frontal	6	-2	14	56	7.01	11,408
	Right	Middle cingulate cortex	32	8	26	38	3.68	
	Left	Posterior-medial frontal	6	-2	4	62	3.20	
3	Right	Middle frontal gyrus	8	48	12	46	3.13	1,904
	Right	Middle frontal gyrus	8	34	16	44	2.82	
	Right	Inferior frontal gyrus	45	58	14	34	2.39	
4	Left	Inferior frontal gyrus	44	-46	16	-4	2.61	1,792
	Left	Inferior frontal gyrus	45	-52	22	2	2.48	
	Left	Inferior frontal gyrus	45	-52	20	-2	2.47	
5	Left	Superior parietal lob-ule	7	-28	-58	50	3.59	1,704
6	Left	Thalamus (temporal)	50	-2	-16	6	2.39	1,016
	Left	Thalamus (prefrontal)	50	-10	-6	-4	2.32	
	Left	Thalamus (prefrontal)	50	-10	-14	4	2.18	
7	Left	Insula lobe	13	-34	26	2	2.84	1,016
8	Right	Insula lobe	13	38	22	-6	3.17	1,000

Table Appendix R. Meta-analytic functional connectivity of SL-specific left MFG cluster. Functional clusters obtained by MACM for left MFG/PCG cluster from the SL comprehension vs. SLA observation contrast, identifying regions that are co-activated with voxels in this cluster in all functional studies in the BrainMap database (containing the results of 3,406 papers describing 16,901 experiments at the time of search). The GingerALE output for this analysis is available as part of the online materials. Mask dimensions = 77 x 96 x 79; number of within-brain voxels = 229,781; number of foci = 1,094; number of experiments = 66; total number of subjects = 960; maximum ALE score (× 10-2) = 19.45; thresholding method = cluster-level inference; thresholding value = .05; number of thresholding permutations = 10,000; cluster-forming value = .001.

Appendix S Functional domains in BrainMap for SLA-specific left PCG cluster

Figure Appendix S. Functional domains in the BrainMap database (containing the results of 3,406 papers describing 16,901 experiments at the time of search) associated with SLA-specific voxels in the left PCG cluster from the SL comprehension vs. SLA observation contrast analysis. Voxels that are part of this cluster observed during non-linguistic SLA observation were also activated in experiments attributed to the five given major domains and sub-domains. The graph indicates the total number of experiments that have been associated with a domain. The Sleuth output for this analysis is available as part of the online materials.

Appendix T Meta-analytic connectivity of SLA-specific left PCG cluster

Cluster	Hemi-sphere	Brain region	BA	MNI Coordinates (mm)			ALE Score ($\times 10^{-2}$)	Cluster Size (mm^3)
				x	y	z		
1	Right	Inferior frontal gyrus	44	50	8	28	41.26	28,704
	Right	Insula lobe	13	36	20	2	11.50	
	Right	Middle frontal gyrus	6	28	-2	56	7.93	
	Right	Middle frontal gyrus	6	34	-2	58	7,58	
	Right	Middle frontal gyrus	9	44	40	22	6.61	
	Right	Inferior frontal gyrus	45	52	22	18	5.28	
	Right	Inferior frontal gyrus	45	46	30	28	4.99	
	Right	Middle frontal gyrus	9	34	44	28	4.00	
2	Left	Inferior frontal gyrus	44	-48	6	28	15.17	17,424
	Left	Middle frontal gyrus	6	-26	-4	50	8.81	
	Left	Precentral gyrus	6	-44	0	44	6.23	
	Left	Inferior frontal gyrus	45	-48	28	16	5.20	
	Left	Middle frontal gyrus	9	-36	38	30	3.69	
3	Left	Posterior-medial frontal	6	0	12	48	12.38	15,184
	Right	Middle cingulate cortex	32	6	24	36	8.65	
4	Left	Inferior parietal lobule	7	-32	-54	50	8.23	15,064
	Left	Superior parietal lob-ule	7	-26	-60	48	8.20	
	Left	Inferior parietal lobule	7	-24	-66	44	8.07	
	Left	Inferior parietal lobule	40	-40	-44	44	7.79	
	Left	Middle occipital gyrus	39	-28	-80	32	6.08	
	Left	Supramarginal gyrus	40	-60	-28	34	5.09	
	Left	Superior parietal lob-ule	7	-12	-72	52	3.46	
5	Right	Angular gyrus	39	30	-64	46	8.77	14,000
	Right	Inferior parietal lobule	7	32	-54	48	8.44	
	Right	Inferior parietal lobule	40	50	-34	46	5.37	
	Right	Supramarginal gyrus	40	42	-38	40	5.23	
6	Left	Thalamus	50	-10	-20	8	6.84	10,560
	Right	Pallidum		16	8	2	6.22	
	Right	Thalamus	50	10	-14	8	6.21	
	Unas-signed			-4	-28	-8	5.61	
	Right	Pallidum		18	0	6	5.15	
	Right	Thalamus	50	8	-28	-6	4.04	
	Unas-signed			4	-26	-4	3.97	
7	Right	Inferior temporal gyrus	37	48	-64	-8	7.94	6,584
8	Left	Inferior temporal gyrus	37	-46	-66	-8	7.39	6,000
	Left	Inferior temporal gyrus	37	-46	-50	-16	4.93	
9	Left	Insula	47	-34	22	2	11.46	5,088
10	Left	Thalamus (prefrontal)		-16	0	12	5.02	2,520
	Unas-signed			-14	4	8	4.90	
11	Right	Middle occipital gyrus	18	32	-86	6	5.10	2,064
	Right	Middle occipital gyrus	18	32	-86	2	4.81	
	Right	Middle occipital gyrus	19	34	-84	18	4.65	
12	Right	Supramarginal gyrus	40	62	-28	26	4.86	1,376
	Right	Supramarginal gyrus	40	56	-32	32	4.56	

Table Appendix T. Meta-analytic functional connectivity of SLA-specific left PCG cluster. Functional clusters obtained by MACM for left PCG cluster from the SLA observation vs. SL comprehension contrast identifying regions that are co-activated with voxels in this cluster in all functional studies in the BrainMap database (containing the results of 3,406 papers describing 16,901 experiments at the time of search). The GingerALE output for this analysis is available as part of the online materials. Mask dimensions = 77 x 96 x 79; number of within-brain voxels = 229,781; number of foci = 3,035; number

of experiments = 120; total number of subjects = 1,886; maximum ALE score (× 10-2) = 41.26; thresholding method = cluster-level inference; thresholding value = .05; number of thresholding permutations = 10,000; cluster-forming value = .001.

References for Appendices

Adamovich SV, August K, Merians A, Tunik E. 2009. A virtual reality-based system integrated with fmri to study neural mechanisms of action observation-execution: a proof of concept study. Restor Neurol Neurosci. 27:209–223.

Amunts K, Schleicher A, Bürgel U, Mohlberg H, Uylings HBM, Zilles K. 1999. Broca's region revisited: Cytoarchitecture and intersubject variability. J Comp Neurol. 412:319–341.

Buccino G, Binkofski F, Fink GR, Fadiga L, Fogassi L, Gallese V, Seitz RJ, Zilles K, Rizzolatti G, Freund H-J. 2001. Action observation activates premotor and parietal areas in a somatotopic manner: an fMRI study: Cortical activation during action observation. Eur J Neurosci. 13:400–404.

Capek CM, Waters D, Woll B, MacSweeney M, Brammer MJ, McGuire PK, David AS, Campbell R. 2008. Hand and mouth: Cortical correlates of lexical processing in British Sign Language and speechreading English. J Cogn Neurosci. 20:1220–1234.

Cardin V, Orfanidou E, Rönnberg J, Capek CM, Rudner M, Woll B. 2013. Dissociating cognitive and sensory neural plasticity in human superior temporal cortex. Nat Commun. 4.

Carr L, Iacoboni M, Dubeau M-C, Mazziotta JC, Lenzi GL. 2003. Neural mechanisms of empathy in humans: A relay from neural systems for imitation to limbic areas. Proc Natl Acad Sci. 100:5497–5502.

Clos M, Amunts K, Laird AR, Fox PT, Eickhoff SB. 2013. Tackling the multifunctional nature of Broca's region meta-analytically: Co-activation-based parcellation of area 44. NeuroImage. 83:174–188.

Corina DP, Chiu Y-S, Knapp H, Greenwald R, San Jose-Robertson L, Braun A. 2007. Neural correlates of human action observation in hearing and deaf subjects. Brain Res. 1152:111–129.

Eickhoff SB, Paus T, Caspers S, Grosbras M-H, Evans AC, Zilles K, Amunts K. 2007. Assignment of functional activations to probabilistic cytoarchitectonic areas revisited. NeuroImage. 36:511–521.

Eickhoff SB, Stephan KE, Mohlberg H, Grefkes C, Fink GR, Amunts K, Zilles K. 2005. A new SPM toolbox for combining probabilistic cytoarchitectonic maps and functional imaging data. NeuroImage. 25:1325–1335.

Emmorey K, Allen JS, Bruss J, Schenker N, Damasio H. 2003. A morphometric analysis of auditory brain regions in congenitally deaf adults. Proc Natl Acad Sci. 100:10049–10054.

Emmorey K, Xu J, Gannon P, Goldin-Meadow S, Braun A. 2010. CNS activation and regional connectivity during pantomime observation: No engagement of the mirror neuron system for deaf signers. NeuroImage. 49:994–1005.

Engel A, Burke M, Fiehler K, Bien S, Rösler F. 2008. How moving objects become animated: The human mirror neuron system assimilates non-biological movement patterns. Soc Neurosci. 3:368–387.

Finkl T, Hahne A, Friederici AD, Gerber J, Mürbe D, Anwander A. 2019. Language without speech: Segregating distinct circuits in the human brain.

Georgescu AL, Kuzmanovic B, Santos NS, Tepest R, Bente G, Tittgemeyer M, Vogeley K. 2014. Perceiving nonverbal behavior: Neural correlates of processing movement fluency and contingency in dyadic interactions: Perceiving Nonverbal Interactive Behavior. Hum Brain Mapp. 35:1362–1378.

Gizewski ER, Lambertz N, Ladd ME, Timmann D, Forsting M. 2005. Cerebellar activation patterns in deaf participants for perception of sign language and written text: NeuroReport. 16:1913–1917.

Grosbras M-H, Paus T. 2006. Brain Networks Involved in Viewing Angry Hands or Faces. Cereb Cortex. 16:1087–1096.

Handjaras G, Bernardi G, Benuzzi F, Nichelli PF, Pietrini P, Ricciardi E. 2015. A topographical organization for action representation in the human brain: Action Topography in the Human Brain. Hum Brain Mapp. 36:3832–3844.

Horan WP, Iacoboni M, Cross KA, Korb A, Lee J, Nori P, Quintana J, Wynn JK, Green MF. 2014. Self-reported empathy and neural activity during action imitation and observation in schizophrenia. NeuroImage Clin. 5:100–108.

Inubushi T, Sakai KL. 2013. Functional and anatomical correlates of word-, sentence-, and discourse-level integration in sign language. Front Hum Neurosci. 7.

Jednoróg K, Bola Ł, Mostowski P, Szwed M, Boguszewski PM, Marchewka A, Rutkowski P. 2015. Three-dimensional grammar in the brain: Dissociating the neural correlates of natural sign language and manually coded spoken language. Neuropsychologia. 71:191–200.

Kilintari M, Narayana S, Babajani-Feremi A, Rezaie R, Papanicolaou AC. 2016. Brain activation profiles during kinesthetic and visual imagery: An fMRI study. Brain Res. 1646:249–261.

Li H, Chen Y, Li Y, Yin B, Tang W, Yu X, Huang W, Geng D, Zhang B. 2015. Altered cortical activation during action observation in amyotrophic lateral sclerosis patients: a parametric functional MRI study. Eur Radiol. 25:2584–2592.

Lorey B, Naumann T, Pilgramm S, Petermann C, Bischoff M, Zentgraf K, Stark R, Vaitl D, Munzert J. 2013. How equivalent are the action execution, imagery, and observation of intransitive movements? Revisiting the concept of somatotopy during action simulation. Brain Cogn. 81:139–150.

MacSweeney M, Campbell R, Woll B, Brammer MJ, Giampietro V, David AS, Calvert GA, McGuire PK. 2006. Lexical and sentential processing in British Sign Language. Hum Brain Mapp. 27:63–76.

MacSweeney M, Campbell R, Woll B, Giampietro V, David AS, McGuire PK, Calvert GA, Brammer MJ. 2004. Dissociating linguistic and nonlinguistic gestural communication in the brain. NeuroImage. 22:1605–1618.

MacSweeney M, Waters D, Brammer MJ, Woll B, Goswami U. 2008. Phonological processing in deaf signers and the impact of age of first language acquisition. NeuroImage. 40:1369–1379.

MacSweeney M, Woll B, Campbell R, McGuire PK, David SA, Williams SCR, Suckling J, Calvert GA, Brammer MJ. 2002. Neural systems underlying British Sign Language and audio-visual English processing in native users. Brain. 125:1583–1593.

Malaia E, Ranaweera R, Wilbur RB, Talavage TM. 2012. Event segmentation in a visual language: Neural bases of processing American Sign Language predicates. NeuroImage. 59:4094–4101.

Martineau J, Andersson F, Barthélémy C, Cottier J-P, Destrieux C. 2010. Atypical activation of the mirror neuron system during perception of hand motion in autism. Brain Res. 1320:168–175.

Mayberry RI, Chen J-K, Witcher P, Klein D. 2011. Age of acquisition effects on the functional organization of language in the adult brain. Brain Lang. 119:16–29.

McCullough S, Saygin AP, Korpics F, Emmorey K. 2012. Motion-sensitive cortex and motion semantics in American Sign Language. NeuroImage. 63:111–118.

McGuire PK, Robertson D, Thacker A, David AS, Kitson N, Frackowiak RSJ, Frith CD. 1997. Neural correlates of thinking in sign language. NeuroReport. 8:695–698.

Moher D, Liberati A, Tetzlaff J, Altman DG, The PRISMA Group. 2009. Preferred reporting items for systematic reviews and meta-analyses: The PRISMA statement. PLoS Med. 6:e1000097.

Montgomery KJ, Haxby JV. 2008. Mirror Neuron System Differentially Activated by Facial Expressions and Social Hand Gestures: A Functional Magnetic Resonance Imaging Study. J Cogn Neurosci. 20:1866–1877.

Montgomery KJ, Isenberg N, Haxby JV. 2007. Communicative hand gestures and object-directed hand movements activated the mirror neuron system. Soc Cogn Affect Neurosci. 2:114–122.

Moreno A, Limousin F, Dehaene S, Pallier C. 2018. Brain correlates of constituent structure in sign language comprehension. NeuroImage. 167:151–161.

Müller VI, Cieslik EC, Laird AR, Fox PT, Radua J, Mataix-Cols D, Tench CR, Yarkoni T, Nichols TE, Turkeltaub PE, Wager TD, Eickhoff SB. 2018. Ten simple rules for neuroimaging meta-analysis. Neurosci Biobehav Rev. 84:151–161.

Newman AJ, Supalla T, Fernandez N, Newport EL, Bavelier D. 2015. Neural systems supporting linguistic structure, linguistic experience, and symbolic communication in sign language and gesture. Proc Natl Acad Sci. 112:11684–11689.

Newman AJ, Supalla T, Hauser P, Newport EL, Bavelier D. 2010. Dissociating neural subsystems for grammar by contrasting word order and inflection. Proc Natl Acad Sci. 107:7539–7544.

Papitto G, Friederici AD, Zaccarella E. 2020. The topographical organization of motor processing: An ALE meta-analysis on six action domains and the relevance of Broca's region. NeuroImage. 206:116321.

Petitto LA, Zatorre RJ, Gauna K, Nikelski EJ, Dostie D, Evans AC. 2000. Speech-like cerebral activity in profoundly deaf people processing signed languages: Implications for the neural basis of human language. Proc Natl Acad Sci. 97:13961–13966.

Pierno AC, Tubaldi F, Turella L, Grossi P, Barachino L, Gallo P, Castiello U. 2009. Neurofunctional Modulation of Brain Regions by the Observation of Pointing and Grasping Actions. Cereb Cortex. 19:367–374.

Plata Bello J, Modroño C, Marcano F, González–Mora JL. 2013. Observation of Simple Intransitive Actions: The Effect of Familiarity. PLoS ONE. 8:e74485.

Plata Bello J, Modroño C, Marcano F, González–Mora JL. 2014. The mirror neuron system and motor dexterity: What happens? Neuroscience. 275:285–295.

Plata-Bello J, Pérez-Martín Y, Castañón-Pérez A, Modroño C, Fariña H, Hernández-Martín E, González-Platas M, Marcano F, González–Mora JL. 2017. The Mirror Neuron System in Relapsing Remitting Multiple Sclerosis Patients with Low Disability. Brain Topogr. 30:548–559.

Sperduti M, Guionnet S, Fossati P, Nadel J. 2014. Mirror Neuron System and Mentalizing System connect during online social interaction. Cogn Process. 15:307–316.

Szameitat AJ, Shen S, Conforto A, Sterr A. 2012. Cortical activation during executed, imagined, observed, and passive wrist movements in healthy volunteers and stroke patients. NeuroImage. 62:266–280.

Trumpp NM, Kiefer M. 2018. Functional reorganization of the conceptual brain system after deafness in early childhood. PLOS ONE. 13:e0198894.

Villarreal M, Fridman EA, Amengual A, Falasco G, Gerscovich ER, Ulloa ER, Leiguarda RC. 2008. The neural substrate of gesture recognition. Neuropsychologia. 46:2371–2382.

Waters D, Campbell R, Capek CM, Woll B, David AS, McGuire PK, Brammer MJ, MacSweeney M. 2007. Fingerspelling, signed language, text and picture processing in deaf native signers: The role of the mid-fusiform gyrus. NeuroImage. 35:1287–1302.

Wheaton KJ, Thompson JC, Syngeniotis A, Abbott DF, Puce A. 2004. Viewing the motion of human body parts activates different regions of premotor, temporal, and parietal cortex. NeuroImage. 22:277–288.